Applied Catalysis A: General 360 (2009) 81–88

Contents lists available at ScienceDirect

Applied Catalysis A: General

journal homepage: www.elsevier.com/locate/apcata

Catalytic oxidation of diesel soot: New characterization and kinetic evidence related to the reaction mechanism on K/CeO_2 catalyst

Martín S. Gross, Maria A. Ulla, Carlos A. Querini *

Instituto de Investigaciones en Catálisis y Petroquímica (INCAPE) – FIQ – UNL – CONICET, Santiago del Estero 2654, Santa Fe S3000AOJ, Argentina

ARTICLE INFO

Article history:
Received 30 January 2009
Received in revised form 3 March 2009
Accepted 6 March 2009
Available online 19 March 2009

Keywords:
Diesel soot
Kinetics
Mechanism
Cerium oxide catalysts

ABSTRACT

The oxidation of diesel soot using K/CeO_2 catalysts is studied in this paper. The reaction system involved in the catalytic oxidation of soot is quite complex; therefore, the study of reaction mechanisms is particularly difficult to address and, consequently, there are few publications related to this topic. In this work, kinetic tests providing new information on this mechanism are shown. Using temperature-programmed oxidation experiments designed in order to get the combustion of only a fraction of the soot, it was possible to observe transient phenomena that demonstrate that the soot oxidation reaction involves many steps and intermediate species. Fourier transform infrared spectroscopy (FTIR), SEM and energy-dispersive X-ray analysis (EDX) characterization results obtained before and after partial burning experiments of soot, also provided information on catalysts morphological changes during the reaction. It was found that peroxide and superoxides associated to CeO_2 are present on the catalyst during soot oxidation. On the other hand, carbonates are formed on the catalyst surface reaching a pseudo-steady-state. The formation of peroxides and superoxides and its surface diffusion explained the transient behavior observed during temperature-programmed experiments designed to burn a fraction of soot under isothermal condition.

1. Introduction

In the last few years, the number of diesel cars has increased, consequently originating a higher concentration of particulate matter (PM) and nitrogen oxides (NO_x) in the urban atmosphere. PM and NO_x are the main contaminants produced by this kind of vehicles. Nevertheless, other contaminants that are present in the exhaust gases of diesel engines are carbon monoxide, hydrocarbons, and sulfur dioxide. Different alternatives and catalysts have been studied in the last two decades in order to reach the maximum limits established by national and international regulations [1–5]. Among the different alternatives proposed, the after-treatment of tail pipe gases with catalytic filters is likely the most promising one. The catalytic elimination of PM is a particularly complex issue. There are three phases involved in this system, two of them are solid (soot and catalyst) and the third one is gas (mainly oxygen and the combustion products: carbon dioxide and water). Since the temperature of tailpipe gases can be as low as 200 °C for light cars or as high as 600 °C for heavy trucks, the catalyst must be active at low temperatures and must have good stability at high temperatures [6]. To favour the contact between the solid phases, catalysts formulated with species with a high mobility are preferred, such as potassium-promoted catalysts [7,8].

The soot–catalyst contact appears to be one of the most important problems to be overcome [9]. It has been proposed that, for laboratory studies, the most realistic method for bringing soot into physical contact with an oxidation catalyst is soot filtration from a diesel-exhaust gas [10]. Other convenient methods recommended by these authors are simply mixing with a spatula, shaking in a sample bottle, dipping in soot dispersion, or filtering from an artificial soot aerosol. These procedures lead to the loose contact mode. The tight contact mode, consists of mixing the catalyst and the soot in a mortar or in a ball mill, and makes it possible to determine intrinsic kinetics. This latter type of mixing procedure has been extensively used to study this catalytic system [11–19].

A large number of catalytic formulations have been tested for the catalytic combustion of diesel soot. Despite of this, the reaction mechanism for this system has been scarcely addressed and therefore a lot of work is still needed in order to advance towards a rational catalyst design. To get information regarding the reaction mechanism and the role that each of the catalyst components plays, intrinsic reaction rates must be evaluated. This means that phenomena like mass and heat transfer limitations must be

* Corresponding author at: Santiago del Estero 2654, (S3000AOJ) Santa Fe, Argentina. Tel.: +54 342 4533858; fax: +54 342 4531068.
E-mail address: querini@fiq.unl.edu.ar (C.A. Querini).

0926-860X/$ – see front matter © 2009 Elsevier B.V. All rights reserved.
doi:10.1016/j.apcata.2009.03.011

minimised. Working under realistic soot–catalyst contact (loose contact), implies that mass transfer limitations become very important, thus decreasing the overall reaction rate. On the other hand, working under tight contact conditions does not represent the situation in a real application, but it is relevant in order to study the intrinsic catalytic chemistry. Thus, results obtained with both types of contacts are useful in laboratory studies.

In this work catalysts containing potassium supported on cerium oxide are studied. The main objective is to determine the reaction mechanism and to learn about the role of each catalytic function. This information can be used to obtain kinetic equations for this system and to improve the fundamental basis for a rational catalytic design. A combination of several techniques such as temperature-programmed oxidation (with various heating rates and final temperatures) and characterization by Fourier transform infrared spectroscopy (FTIR), SEM, energy-dispersive X-ray analysis (EDX) and X-ray diffraction (XRD) are used to reach the proposed objective.

2. Experimental

2.1. Soot, catalysts, and catalyst:soot mixtures preparation

Soot was obtained by burning commercial diesel fuel as described in [7]. The soot was collected from the recipient walls and then was dried in a stove at 120 °C for 24 h.

The catalysts were prepared from suspensions of cerium (IV) oxide in aqueous solution of potassium nitrate. The amount of nitrate solution was the necessary to obtain catalysts with 4, 7, 10 and 14 wt% of potassium referred to cerium oxide. The mixture was evaporated until achieving a paste, which was dried in a stove for 24 h at 120 °C and then calcined at 450 °C.

In this work, catalysts and soot were mixed with a mass ratio of 20:1. To prepare these mixtures, the weighted solids were placed in a mortar and were mechanically mixed for 6 min (tight contact). This mixing procedure has been extensively used in laboratory studies [20,6,21].

2.2. Catalysts activity

Catalytic activity was determined by temperature-programmed oxidation (TPO) tests, carried out with the catalyst:soot mixtures prepared as above described. The amount of sample loaded into the cell was 10 mg. Different temperature programmes were used in the TPO experiments. A set of experiments was carried out using different heating rates, e.g., 4, 8, 12 and 16 °C/min. A second set of experiments consisted in heating the sample at 12 °C/min until a given pre-selected temperature was reached, and then holding this temperature for a given time. Finally, another set of TPO experiments was carried out heating the sample in an inert gas flow (N_2) until a given temperature was reached. At this moment the gas was switched to an O_2/N_2 mixture holding a constant temperature. In all cases, the gas flow rate and composition were the same, 25 cm^3/min and 6% O_2 (N_2 to balance) respectively. The gases coming out of the reaction cell went through a methanation reactor where the CO and CO_2 were converted to CH_4 with 100% conversion [22]. This reactor operated at 400 °C, and was loaded with a nickel catalyst. Methane formed in this reactor was continuously monitored with a FID.

In order to verify that the catalytic bed temperature closely follows the selected temperature program and no energy transfer limitations take place, several experiments were carried out. The cell is a straight quartz tube with 7 mm outer diameter. Three thermocouples were used. One of them was located on the outer surface of the reactor wall, connected to the temperature controller. The other two were placed inside the reactor, one directly in the catalytic bed, and the other one right below it. These two thermocouples did no show any difference between them during the run. The difference between the external thermocouple and the one located in the bed was at most 5 °C, being this difference constant during the ramp, and the time needed to fully equilibrate once the final value was reached was less than 1 min.

The selection of the experimental variables used to perform the temperature-programmed oxidation analysis were carefully selected, checking that there was no detectable temperature increase in the bed due to the exothermic reaction, or mass transfer limitations. This study was recently sent for publication [21]. A systematic study of the influence of gas carrier flow rate, catalyst:soot mass ratio, sample mass loaded to the cell, and mixing time, allowed us to select the experimental values of the variables associated to this analysis.

2.3. Catalyst characterization

Catalysts samples after being used in TPO experiments and soot–catalyst mixtures after partial burning experiments at different final temperatures were characterized by FTIR and XRD. Infrared spectra were obtained using an IRPrestige-21 Shimadzu spectrometer. Samples were prepared in the form of pressed wafers (ca. 1% sample in KBr). All spectra involved the accumulation of 80 scans at 8 cm^{-1} resolution. Crystalline phases were identified by powder XRD analysis using a Shimadzu XD-D1 diffractometer, equipped with a Cu Kα radiation source and using a scanning rate of 1 min^{-1}. The morphology of soot–catalyst mixtures, both just-prepared and after partial burnt experiments was examined by Scanning Electron Microscopy (JEOL JSM 35C) operated at 20 kV. The atomic elemental analyses were obtained using an EDX system attached to the SEM instrument.

3. Results and discussion

3.1. Influence of catalyst composition on the activity

Fig. 1 shows the TPO profiles for the catalysts with different potassium loadings, in the range 4–14 wt%. The heating rate used in these experiments was 12 °C/min. The temperature that corresponds to the maximum in the TPO profiles (TM) is plotted in Fig. 2 as a function of the K content. It can be clearly seen that there is an optimum composition in K loading for which the temperature, TM, associated to the maximum is the lowest. The

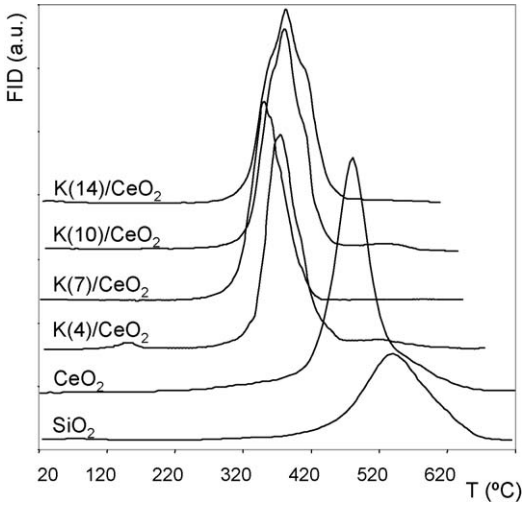

Fig. 1. TPO profiles corresponding to K(x)/CeO_2 catalysts with different K loadings, unpromoted ceria, and non-catalyzed soot combustion.

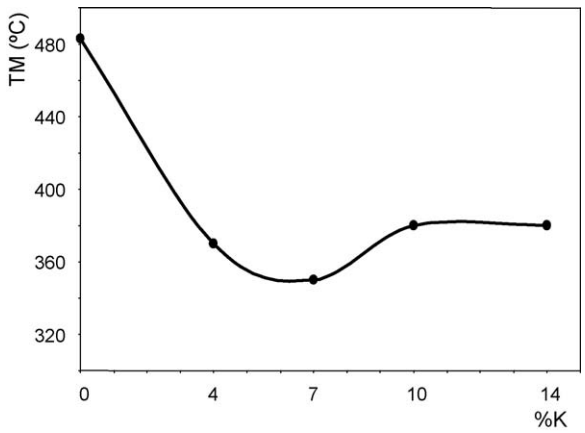

Fig. 2. Temperatures corresponding to the maximum in the TPO profiles (TM) as a function of K loading.

unpromoted catalyst has very low activity, with a maximum in the TPO profile at 480 °C, while when the soot is deposited on an inert material (e.g., silica) the maximum is displayed at 540 °C. These results agree with similar findings reported by Aneggi et al. [6].

The most active catalyst is the one that contains 7 wt% of K. These results suggest that there is a Ce:K ratio for which the synergism is maximum, leading to the most active catalyst. It has been reasonably established [23,24] that K improves the catalyst activity due to its high mobility, favouring the contact with soot. Therefore, at low K loadings, this component is the one that limits the overall reaction rate. On the other hand, at high K loadings the catalyst surface is fully covered by this compound, and under this condition not enough CeO_x is exposed to the gas phase. This oxide provides the oxygen needed for the oxidation of soot and is reoxidized by the oxygen present in the gas phase, due to its well-known redox properties [25]. Therefore, from the mechanistic point of view, at high K loadings these reoxidation steps are the controlling ones.

In Fig. 1, it also can be seen that the combustion start at different temperatures depending upon the potassium content. The onset of the oxidation starts at lower temperature for the catalyst that contains 7 wt% K.

3.2. Kinetic parameters

Even though in this work we are presenting evidence about the complexity of the kinetics involved in the soot oxidation, simplified models can still be used to obtain a global representation of the system, particularly the global activation energy.

A power law kinetic model has been used in many publications. We used it in this catalytic system, to evaluate the expected effect of the experimental variables on the TPO profile [21]. In this model, the expose surface concentration of carbon was used in the rate expression and a reaction order less than one was considered to take into account that the soot particles are initially three-dimensional.

It is possible to estimate this energy by using the following expression:

$$\ln(r) = \ln(A) + \ln(f(C,P)) + \frac{E}{R}\cdot\frac{1}{T} \quad (1)$$

where r is the reaction rate, $f(C,P)$ is a function that includes the dependence of the reaction rate on soot concentration, oxygen partial pressure and soot particle geometry. It is assumed that the global kinetic constant follows the Arrhenius law, A being the pre-exponential factor, E the activation energy and R the universal gases constant. The global activation energy can be obtained using a set of soot combustion reactions under isothermal conditions, at several temperatures, and measuring the reaction rate at different conversion levels. This is easily accomplished with our experimental setup, where a continuous monitoring of the FID signal is obtained, being this signal directly proportional to the reaction rate (r). This proportionality constant is obtained by calibration with pulses of known amounts of CO_2.

Experimental values of the reaction rate obtained at 50% conversion for three catalysts with different K content are plotted as a function of $(1/T)$ in Fig. 3. This level of conversion was chosen in order to have both good sensitivity, and also to decrease the possibility of mass and energy transfer limitations. It has to be considered that the 50% conversion is reached after some time at constant temperature, and since the soot amount decreased to half of the initial value, the reaction rate will correspondingly be the half of the initial value. Then, the instantaneous reaction rate decreases as the soot conversion increases, and therefore there will be less problems associated to mass transfer limitations and high heat release, as compared to the situation at low soot conversion. Table 1 presents the activation energy values determined from these data with this simplified kinetic model. The tendency of activation energies obtained from these experiments at constant temperature is in agreement with results shown in Figs. 1 and 2, where it was shown that the $K(7)/CeO_2$ catalyst is the most active among those studied in this work, and correspondingly, the one with lower global activation energy. Activation energies reported in Table 1 agree with values reported by other research groups. For example, Fino et al. [26] reported a value of 129.25 kJ/mol, using a perovskite as catalyst. For the uncatalyzed reaction activation energies of 137 [27], 163 [28] and 164 kJ/mol [29] were reported, while using CeO_2 and carbon black it was reported a value of 90 kJ/mol [28]. Using $Pt/CeZrO_2$ the activation energy was 114 kJ/mol [29]. The value that we found for $K(7)/CeO_2$ is lower than most of the reported values for other catalysts, what means that this catalyst has a very good activity.

3.3. Catalyst stability

Catalyst stability was explored by carrying out successive TPO experiments using the same catalyst sample to mix with soot. It was found that TM was the same in successive TPO experiments (not shown).

The catalyst was analyzed by FTIR before and after each reaction cycle. The results are shown in Fig. 4. The FTIR spectrum that corresponds to the fresh catalyst is different from those obtained after each reaction cycle. The main vibrational bands in the fresh sample spectrum are a sharp signal at 1385 cm^{-1} and a small one at 830 cm^{-1}, both of them attributed to nitrate species (Fig. 4, solid line). However, seven new signals are observed in the IR spectrum

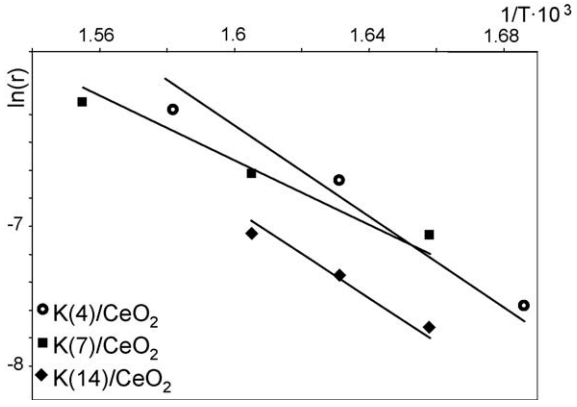

Fig. 3. Arrhenius plots for $K(x)/CeO_2$: x = 4, 7 and 14%.

Table 1
Global activation energies.

Catalyst	E (kJ/mol)
K(4)/CeO_2	108.7
K(7)/CeO_2	73.9
K(14)/CeO_2	105.8

obtained with the sample after the first cycle: 1640, 1430 (shoulder), 1272, 1124, 1010, 870 and 705 cm^{-1} (Fig. 4, dotted line). The broad band observed at 1640 cm^{-1} corresponds to the flexion vibrational mode of adsorbed water molecules.

The bands at 1430, 1010 and 705 cm^{-1} which correspond to carbonates species clearly show that these kinds of compounds are formed during soot combustion. Most probably, the signals correspond to potassium carbonate. On the other hand, it can be inferred that carbonates are formed from nitrates, since the band at 1385 cm^{-1} (attributed to nitrates) decreases in intensity when comparing the fresh and the used catalysts. The decomposition of nitrate species during the soot oxidation is also confirmed by the appearance of monodentated nitrite (NO_2^-) band at 1272 cm^{-1}.

The band at 1124 cm^{-1} is assigned to an adsorbed superoxide species and the very weak band at 883 cm^{-1} is assigned to surface peroxides, both species being associated with CeO_2 [30,31]. The formation of these species could take place during the reaction, in which the partial reduction of Ce^{4+} to Ce^{3+} by carbon (soot) would occur at the same time that O_2 from the gas phase would react with the surface vacancies forming Ce^{3+}–O_2 complexes [32].

The spectra obtained after the first and the second cycle are almost identical, and therefore it can be concluded that the catalyst reaches a steady-state concerning the most relevant species, for example, carbonates or carbonate-type compounds produced via chemisorbed CO_2. These compounds could be formed and decomposed in a range of intermediate temperatures, such as the soot oxidation temperatures. This is a key point, since if these compounds do not decompose, the catalytic surface would be enriched in carbonates composition and a deactivation could be observed. We had previously proposed that the soot oxidation reaction proceeds on these catalysts by a mechanism that involves the formation of a carbonate or more properly said, a complex involving CO_2 and the active components in the catalyst [20,24,33]. We have shown that the active catalyst interacts with CO_2 stronger at temperatures close to 400 °C than at room temperature, what clearly indicates that it is an activated adsorption. If no desorption occurs, then the active site would become saturated and consequently deactivated.

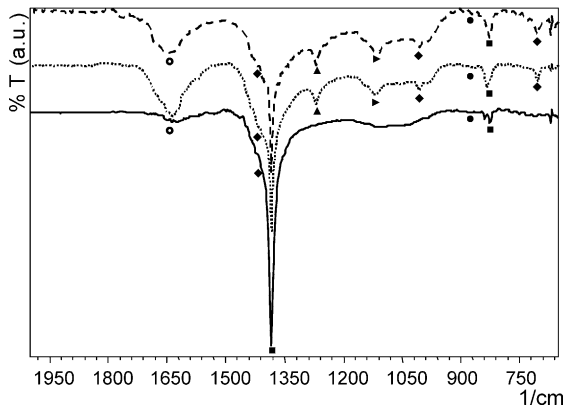

Fig. 4. FTIR spectra for two successive combustion cycles with K(7)/CeO_2 as catalyst: solid line, fresh catalyst; dotted line, after first cycle; dash line, after second cycle. (○) Water; (◆) carbonate; (■) nitrate; (▲) nitrite; (▶) superoxide; (●) peroxide.

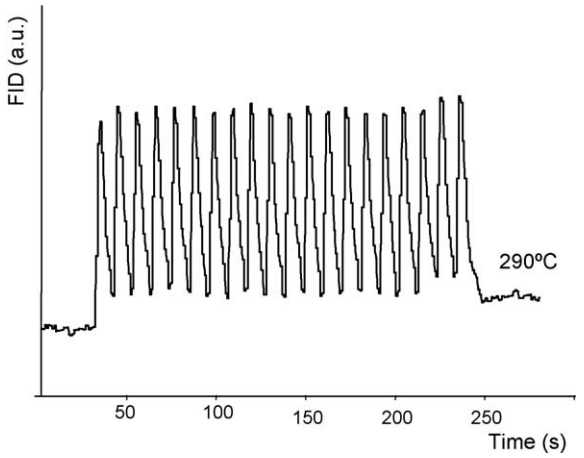

Fig. 5. High frequency CO_2 pulses at different temperatures with K(7)/CeO_2.

This interaction between CO_2 and catalyst surface at different temperatures can be analyzed using the high frequency CO_2 pulses experiment, which is a transient technique that provides information regarding the reversibility of the interaction between the CO_2 and the catalytic surface [34]. Fig. 5 shows as an example, the result obtained at 290 °C. It can be seen that at this temperature the high frequency CO_2 pulses display constant oscillation amplitude. Same type of response was observed at 350 and 450 °C (not shown). All of these responses, have smaller amplitude than the blank experiment, suggesting that the system reaches a pseudo-steady-state and the CO_2 adsorption–desorption process is very fast [33]. Taking the oscillation amplitude of the blank experiment as reference, the amplitude at 250 °C was 89.6% of this reference and at 350 and 450 °C the amplitudes were 70.4 and 59.3% respectively. These results show strong evidence about the catalyst capacity of adsorbing the CO_2 at high temperatures (in the range in which the soot is burnt) and also that it is released from the surface essentially at the same rate. The combined effect is that the surface reaches a steady-state regarding to the CO_2 composition.

3.4. Partial burnt experiments

To obtain information referred to the kinetic mechanism, temperature-programmed oxidation experiments using different intermediate final temperatures were carried out. These values were selected around the temperature that corresponds to the maximum in the TPO profiles (TM) of each catalyst (Fig. 1). In the case of the K(7)/CeO_2 catalyst, this range is 300–350 °C. Fig. 6a shows the result of the experiment obtained with this catalyst. In this experiment the catalyst:soot sample was heated from room temperature up to 320 °C, and then the temperature was held at this value. An unexpected result was obtained. While the typical response for isothermal soot combustion is an exponential reaction rate decay, in this experiment when the temperature of 320 °C was reached, the reaction rate kept increasing for a certain time, reached a maximum, and then decreased. On the other hand, when the final temperature was 350 °C (Fig. 6b), this phenomenon was not observed. The same type of experiments was carried out with the catalysts containing 4, 10, and 14 wt% of K respectively. Fig. 6c shows the results obtained with a final temperature equal to 350 °C. The above mentioned phenomenon was not observed for these latter catalysts in any of these experiments, neither with a final temperature of 350 °C nor at 320 °C (for clarity reasons only results obtained at 350 °C are shown). However, it has been observed with other catalysts not

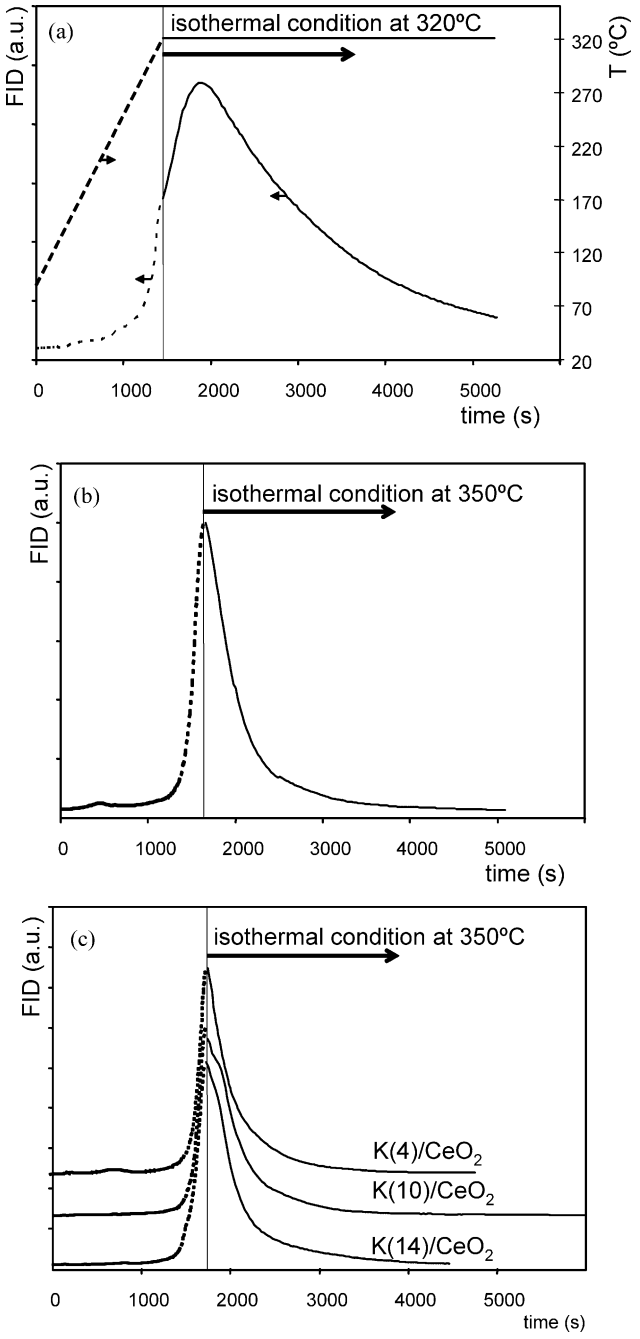

Fig. 6. Combustion at different final temperatures. Dotted line: heating at 12 °C/min, solid line: constant temperature. (a) K(7)/CeO_2 at 320 °C; (b) K(7)/CeO_2 at 350 °C; (c) K(4), K(10) and K(14)/CeO_2 at constant temperature of 350 °C.

included in this work. It has also been verified in many experiments, carried out in order to make sure that this observation is not masked by temperature gradients, and energy or mass transfer limitations. Fig. 6a shows the temperature measured during the TPO experiment. It can be seen that there is no appreciable delay in the bed temperature that could mask the kinetic response. Clearly, the temperature is at a constant level while the signal keeps increasing for a long time.

Taking into account that catalyst modifications occur during the reaction, surface and bulk characterizations were also carried out for the catalysts after partial burnt experiments. Catalyst:soot mixtures were heated up to a given final temperature, and then cooled down very fast in an inert atmosphere, and store in a sealed

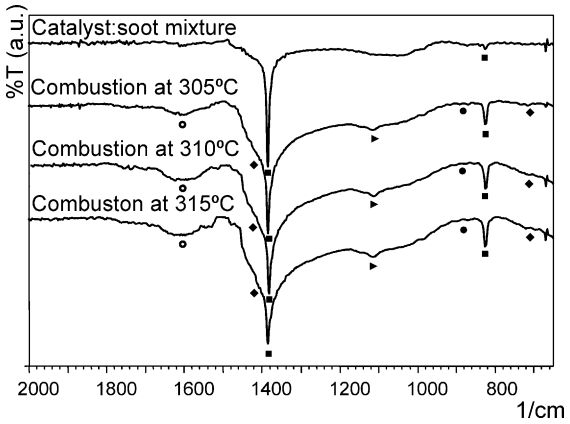

Fig. 7. FTIR spectra of partial combustion at different temperatures. (○) Water; (◆) carbonate; (■) nitrate; (▶) superoxide; (●) peroxide.

vial. These samples were analyzed by FTIR, SEM, and EDX. Fig. 7 shows the FTIR spectra after soot oxidation at 305, 310, and 315 °C, and the spectrum that corresponds to the fresh catalyst.

In the case of the latter, only the signals due to KNO_3 are observed (1385 and 830 cm^{-1}) indicating that the soot has no signal in this range of wave numbers.

On the other hand, the FTIR spectra obtained with the catalyst:soot mixtures after partial burnt experiments, display as the main signal the one associated to KNO_3. However, bands that correspond to carbonates species (1430 and 706 cm^{-1}), the water flexion vibrational mode (1640 cm^{-1}), superoxide species (1124 cm^{-1}) and surface peroxides (883 cm^{-1}) [30,31] start to develop with increasing intensities as final temperature increases, although there are no appreciable differences between spectra at 310 and 315 °C. These results agree with those shown in Fig. 4, obtained after complete soot burning.

SEM micrographs are shown in Fig. 8. In these micrographs, the small white spheres correspond to the soot particles, and cover most of the active phase, which contains potassium species that appear in these pictures as smooth surfaces. As the reaction proceeds, larger areas of potassium active species are observed.

EDX analyses were carried out in two regions of the system, labeled A and B in Fig. 8a. In the first (region A) the potassium content is 5%, while in B it is 32%. These results suggest that highly mobile potassium species contact the soot and oxidize it, as previously suggested [7,8]. Unfortunately, the SEM photos have to be taken at room temperature and therefore the catalytic surface is not the same as during the reaction. Nevertheless, it can be inferred with this micrographs, that at high temperature the potassium components in a highly mobile state accommodate underneath or nearby the soot particles, thus providing the active sites for the oxidation. We do not have further evidence in order to guess whether the K compounds migrate on top of the soot particles or not.

Finally, the samples were characterized by XRD, and the results are shown in Fig. 9 for K(4), K(7), K(10) and K(14)/CeO_2 catalysts. At low K concentration (4 and 7 wt%), only the signals that correspond to CeO_2 are found with a face-centered cubic structure, with peaks at 28.5°, 33.1°, 47.6°, 56.5°, 59.2°, 69,5°, 76,8°, and 79,1°, that correspond to (1 1 1), (2 0 0), (2 2 0), (3 1 1), (2 2 2), (4 0 0), (3 3 1) and (4 2 0) planes respectively (card JCPDS-ICDD 78-694 Rad. Cu $K\alpha_1$). Since no signals due to nitrates are found, it can be concluded that it is well dispersed on the surface. When the concentration of K is higher (10 and 14 wt%) peaks due to KNO_3 can be seen at 23.54°, 23.86°, 29.45°, 33.67°, 33.86°, 34.06°, 41.18°, 43.71°, 44.18° and 46.65°, that correspond to (1 1 1), (0 2 1), (0 1 2), (1 3 0), (1 1 2), (0 2 2), (2 2 1), (2 0 2), (1 3 2) and (1 1 3) planes respec-

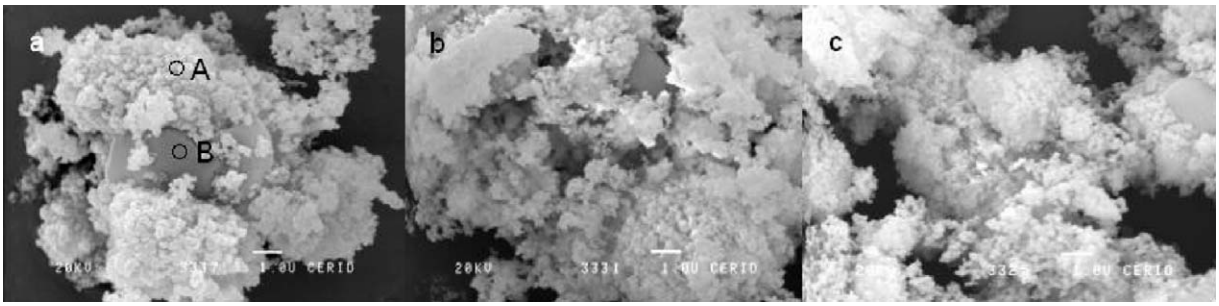

Fig. 8. SEM micrographs of partial combustion at different temperatures: (a) 305 °C; (b) 310 °C; (c) 315 °C.

tively (card JCPDS-ICDD 5-377 Rad. Cu $K\alpha_1$). For the highest K concentration (K(14)/CeO_2) the peaks are more intense than K(10)/CeO_2.

3.5. Reaction mechanism

These results indicate that the reaction rate is not really well represented by a power-law kinetic model, even though the latter has been extensively used in literature [26–29,35–41]. Clearly, there are several steps in the reaction mechanism, in such a way that the reaction pathway goes through intermediate compounds whose concentration finally determines the overall reaction rate. Results obtained with K(7)/CeO_2 catalysts, with a maximum in reaction rate at a given constant temperature cannot be predicted or adjusted with the simplified power law model.

Based on the above described evidence, the following steps can be considered in the reaction mechanism in this system:

- CeO_2 reduction (by soot particles).
- Oxygen diffusion on the surface.
- Oxygen vacancies diffusion.

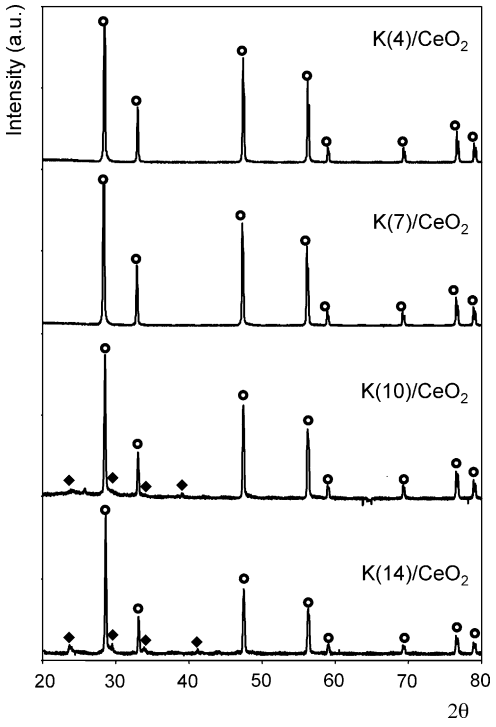

Fig. 9. X-ray diffractograms of K(x)/CeO_2 catalysts. (○) Cerium oxide; (◆) potassium nitrate.

- Vacancies generated by influence of potassium.
- Potassium species diffusion, modifying the contact with the soot as a function of time.
- CeO_2 reoxidation by gas phase oxygen.

Scheme 1 shows the different reaction steps involved in the soot catalytic oxidation with the catalyst used in this study.

Considering this analysis, and literature information regarding CeO_2 chemistry, the following mechanism is proposed:

$$n\mathrm{CeO}_x + \mathrm{O}_2 \rightarrow [n\mathrm{CeO}_x]^{+}\mathrm{O}_2^{-} \quad (2)$$

$$[n\mathrm{CeO}_x]^{+}\mathrm{O}_2^{-} \rightarrow [n\mathrm{CeO}_x]^{2+}\mathrm{O}_2^{2-} \quad (3)$$

$$[n\mathrm{CeO}_x]^{2+}\mathrm{O}_2^{2-} \leftrightarrow n\mathrm{CeO}_y \quad (4)$$

$$2\mathrm{KNO}_3 + C + \tfrac{1}{2}[n\mathrm{CeO}_x]^{2+}\mathrm{O}_2^{2-} \rightarrow \mathrm{K}_2\mathrm{CO}_3 + 2\mathrm{NO}_{2(\mathrm{ads})[n\mathrm{CeO}_x]^{2+}}{}^{-} \quad (5)$$

$$\mathrm{K}_2\mathrm{CO}_3 \leftrightarrow \mathrm{K}_2\mathrm{O} + \mathrm{CO}_2 \quad (6)$$

$$\mathrm{K}_2\mathrm{O} \rightarrow \mathrm{K}_2\mathrm{O}^{*} \quad (7)$$

$$\mathrm{K}_2\mathrm{O}^{*} + \mathrm{NO}_{2(\mathrm{ads})}{}^{-} + [n\mathrm{CeO}_x]^{2+}\mathrm{O}_2^{2-} \rightarrow 2\mathrm{KNO}_3 + [n\mathrm{CeO}_x]^{2+}[]^{2-} \quad (8)$$

$$[n\mathrm{CeO}_x]^{2+}\mathrm{O}_2^{2-} + \mathrm{C}^{*} \rightarrow [n\mathrm{CeO}_x]^{2+}[]^{2-} + \mathrm{CO}_2 \quad (9)$$

$$[n\mathrm{CeO}_x]^{2+}[]^{2-} \leftrightarrow n\mathrm{CeO}_x \quad (10)$$

Steps (2) and (3) correspond to the formation of superoxides and peroxides by CeO_2 oxidation. Peroxide then reacts with soot represented by step (5) involving KNO_3, and forming the potassium carbonate intermediate that then decomposes according to (6). The formation of NO_2^- is proposed based on FTIR results as shown above. Step (7) represents the surface diffusion of potassium compounds, which then reacts with nitrite involving peroxide according to (8). Reaction (9) represents the direct oxidation of soot by peroxide that can diffuse on the surface, generating oxygen vacancies on the ceria surface.

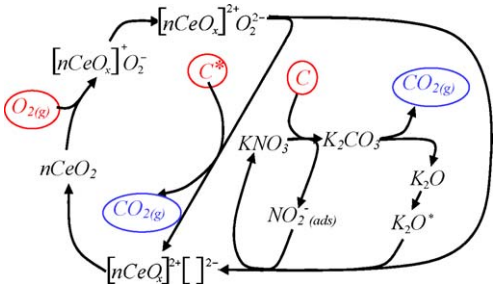

Scheme 1. Reaction network for soot oxidation on K/CeO_2 catalysts.

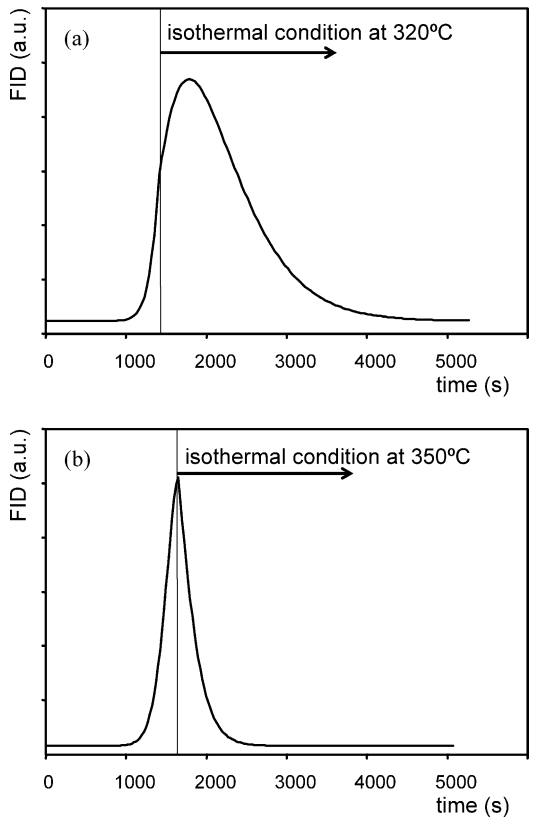

Fig. 10. Simulated temperature-programmed oxidation profiles corresponding to K(7)/CeO_2 catalyst with final temperatures of (A) 320 °C and (B) 350 °C. Kinetic parameters were obtained from the TPO profile shown in Fig. 1.

Taking into account these steps, the rate expression for soot oxidation was written, and it was possible to obtain and predict kinetic responses like those shown in Fig. 6a, with a maximum in the reaction rate at constant temperature. It is possible also to qualitatively analyze the reasons why the reaction rate follows the patterns shown in Fig. 6. The soot oxidation (reaction (5)) involves the formation of superoxide and peroxide (reactions (2) and (3)). At low temperature (e.g., 320 °C), the maximum concentration of these intermediates is reached after some time, and therefore, the reaction rate increases during this evolution. At higher temperatures, such as 350 °C, the maximum concentration of these intermediates has already been reached, and therefore the reaction rate at constant temperature decreases monotonically. Fig. 10 shows the results of the simulation carried out with parameters obtained from the TPO shown in Fig. 1 for K(7)/CeO_2. The model can predict the different behaviors found experimentally with final temperatures of 320 °C and 350 °C. This is a proof of the excellent agreement between the experimental results and the prediction capability of the model developed in this work. It has to be emphasized, that the kinetic parameters were obtained using a standard TPO experiment, and then these parameters where used to predict the responses in experiments using low final temperatures, as those shown in Fig. 6 (experimental) and Fig. 10 (simulated). The values of the parameters for all the catalysts used in this study, and the kinetics equations developed based on the above detailed mechanism will be presented in another study to be published soon.

Additional work is being carried out to include the effect of different precursors such as potassium hydroxide, carbonate, chloride, or nitrate, in the reaction mechanism and therefore to contribute to the understanding of the fundamentals associated with this reaction system.

4. Conclusions

The K(7)/CeO_2 catalyst has the best activity for soot catalytic combustion as compared to the other potassium/ceria catalysts presented in this work. In those cases in which the catalyst is prepared with potassium nitrate as precursor, during the reaction the surface composition changes from its initial state to another one where the surface is partially hydrated and carbonated. However, in spite of these modifications in surface morphology and composition, the activity does not change.

Properly designed TPO experiments, allowed the observation of a phenomenon not reported so far, which is an increase in the soot oxidation rate at constant temperature. These results demonstrate that the power law kinetic applied to this system in many studies is not correct, even though it might be used to obtain global parameters for comparison purposes. It is necessary to include different steps in the reaction mechanism to reproduce the experimental observation, i.e., the increase in reaction rate at constant temperature. These steps include for example the generation of highly active cerium peroxide–superoxide species, support reduction and oxidation steps, surface diffusion of potassium species and the reaction between surface oxygen and carbon (soot). This sequence generates a reaction mechanism in which the formation of active reaction intermediates allows the modeling of the complex phenomena observed such as those shown in Fig. 7. These results are contribution to the understanding of the reaction mechanism, and it can also be expected to contribute towards a more rational catalyst design.

References

[1] G.S. Son, S. Si, US Patent 7,316,106, (2008).
[2] W. Zhang, J.A. Imes, T.R. Taubert, T.L. Ricke, T.G. Angelo, US Patent 7,340,888, (2008).
[3] M.V. Twigg, US Patent 7,404,933, (2008).
[4] M. Pfeifer, B. van Stetten, C. Kühn, R. Staab, L.M. Ruwisch, P. Kattwinkel, J. Geishoff, E. Lox, T. Kreuzer, US Patent 7,351,382, (2008).
[5] M.D. Hemingway, W.J. LaBarge, H. Simpkins, US Patent 7,402,292, (2008).
[6] E. Aneggi, C. de Leitenburg, G. Dolcetti, A. Trovarelli, Catal. Today 136 (2008) 3.
[7] C.A. Querini, M.A. Ulla, F. Requejo, J. Soria, U.A. Sedrán, E.E. Miró, Appl. Catal. B 15 (1998) 5.
[8] C.A. Querini, L.M. Cornaglia, M.A. Ulla, E.E. Miró, Appl. Catal. B 20 (1999) 165.
[9] V. Serra, G. Saracco, C. Badini, V. Specchia, Appl. Catal. B: Environ. 11 (1997) 329.
[10] B.A.A.L. van Setten, J.M. Schouten, M. Makkee, J.A. Moulijn, Appl. Catal. B: Environ. 28 (2000) 253.
[11] D. Fino, N. Russo, G. Saracco, V. Specchia, Top. Catal. 30 (2004) 251.
[12] A. Setiabudi, J. Chen, G. Mul, M. Makkee, J.A. Moulijn, Appl. Catal. B: Environ. 51 (2004) 9.
[13] A. Setiabudi, M. Makkee, J.A. Moulijn, Appl. Catal. B: Environ. 42 (2003) 35.
[14] S. Kureti, W. Weisweiler, K. Hizbullah, Appl. Catal. B: Environ. 43 (2003) 281.
[15] S. Wang, B.S. Haynes, Catal. Commun. 4 (2003) 591.
[16] R. Flouty, E. Abi-Aad, S. Siffert, A. Aboukaïs, Appl. Catal. B: Environ. 46 (2003) 145.
[17] G. Neri, G. Rizzo, S. Galvagno, A. Donato, M.G. Musolino, R. Pietropaolo, Appl. Catal. B: Environ. 42 (2003) 381.
[18] P. Ciambelli, V. Palma, P. Russo, S. Vaccaro, J. Mol. Catal. A: Chem. 204 (2003) 673.
[19] S. Liu, A. Obuchi, J. Uchisawa, T. Nanba, S. Kushiyama, Appl. Catal. B: Environ. 37 (2002) 309.
[20] M.A. Peralta, V.G. Milt, L.M. Cornaglia, C.A. Querini, J. Catal. 242 (2006) 118.
[21] M.A. Peralta, M.S. Gross, M.B. Patiño, C.A. Querini, Chem. Eng. J., submitted for publication.
[22] S.C. Fung, C.A. Querini, J. Catal. 138 (1992) 240.
[23] E.E. Miró, F. Ravelli, M.A. Ulla, L.M. Cornaglia, C.A. Querini, Catal. Today 53 (1999) 631.
[24] M.L. Pisarello, V. Milt, M.A. Peralta, C.A. Querini, E.E. Miró, Catal. Today 75 (2002) 465.
[25] A. Bueno-López, K. Krishna, B. van der Linden, G. Mul, J.A. Moulijn, M. Makkee, Catal. Today 121 (2007) 237.
[26] D. Fino, P. Fino, G. Saracco, V. Specchia, Appl. Catal. B: Environ. 43 (2003) 243.
[27] A. Yezerets, N.W. Currier, D.H. Kim, H.A. Eadler, W.S. Epling, C.H.F. Peden, Appl. Catal. B 61 (2005) 120.
[28] M.N. Bokova, C. Decarne, E. Abi-Aad, A.N. Ptykhin, V.V. Lunin, A. Aboukäis, Thermochim. Acta 428 (2005) 165.
[29] P. Darcy, P. Da Costa, H. Mellottée, J.M. Trichard, G. Djéga-Mariadassou, Catal. Today 119 (2007) 252.

[30] V. Pushkarev, V. Kovalchuk, J. d'Itri, J. Phys. Chem. B 108 (2004) 534.
[31] M. Daturi, E. Finocchio, C. Binet, J.-C. Lavalley, F. Fally, V. Perrichon, H. Vidal, N. Hickey, J. Kaspar, J. Phys. Chem. B 104 (2000) 9186.
[32] A.J. Dyakonov, C.A. Little, App. Catal. B 67 (2006) 52.
[33] V.G. Milt, M.L. Pisarello, E.E. Miró, C.A. Querini, Appl. Catal. B 41 (2003) 397.
[34] V.G. Milt, C.A. Querini, E.E. Miró, Thermochim. Acta 404 (2003) 177.
[35] P. Ciambelli, P. Corbo, M. Gambino, V. Palma, S. Vaccaro, Catal. Today 27 (1996) 99.
[36] J.P.A. Neeft, T.X. Nijhuis, E. Smakman, M. Makkee, J.A. Moulijn, Fuel 76 (1997) 1129.
[37] C. Li, T.C. Brown, Carbon 39 (2001) 725.
[38] F. Larachi, K. Belkacemi, S. Hamoudi, A. Sayari, Catal. Today 64 (2001) 163.
[39] V. Slovák, Thermochim. Acta 372 (2001) 175.
[40] G.A. Stratakis, A.M. Stamatelos, Combust. Flame 132 (2003) 157.
[41] T.J. Keskitalo, K.J.T. Lipiäinen, A.O.I. Krause, Chem. Eng. J. 120 (2006) 63.